Naval Surface Warfare Center
Carderock Division
West Bethesda, MD 20817-5700

NSWCCD-61-TR–2006/01   February 2006

Survivability, Structures, and Materials Department

Technical Report

A Study on the Tensile and Fracture Toughness Behavior of Pure Rhenium Metal

by
Amy C. Robinson
Xian J. Zhang
Brian P. L'Heureux
Jennifer G. Gaies

Naval Surface Warfare Center
Carderock Division
West Bethesda, MD 20817-5700

A Study on the Tensile and Fracture Toughness Behavior of Pure Rhenium Metal

by
Amy C. Robinson
Xian J. Zhang
Brian P. L'Heureux
Jennifer G. Gaies

This page intentionally left blank

REPORT DOCUMENTATION PAGE		*Form Approved* *OMB No. 0704-0188*
Public reporting burden for this collection of information is estimated to average 1 hour per response, including the time for reviewing instructions, searching existing data sources, gathering and maintaining the data needed, and completing and reviewing this collection of information. Send comments regarding this burden estimate or any other aspect of this collection of information, including suggestions for reducing this burden to Department of Defense, Washington Headquarters Services, Directorate for Information Operations and Reports (0704-0188), 1215 Jefferson Davis Highway, Suite 1204, Arlington, VA 22202-4302. Respondents should be aware that notwithstanding any other provision of law, no person shall be subject to any penalty for failing to comply with a collection of information if it does not display a currently valid OMB control number. **PLEASE DO NOT RETURN YOUR FORM TO THE ABOVE ADDRESS.**		

1. REPORT DATE (DD-MM-YYYY) 04/25/2006	2. REPORT TYPE Final	3. DATES COVERED *(From - To)* 4/1/2005 – 12/31/2005
4. TITLE AND SUBTITLE A Study on the Tensile and Fracture Toughness Behavior of Pure Rhenium Metal		5a. CONTRACT NUMBER
		5b. GRANT NUMBER
		5c. PROGRAM ELEMENT NUMBER
6. AUTHOR(S) Amy C. Robinson Xian J. Zhang Brian P. L'Heureux Jennifer G. Gaies		5d. PROJECT NUMBER
		5e. TASK NUMBER
		5f. WORK UNIT NUMBER
7. PERFORMING ORGANIZATION NAME(S) AND ADDRESS(ES) AND ADDRESS(ES) NAVAL SURFACE WARFARE CENTER CARDEROCK DIVISION 9500 MACARTHUR BLVD WEST BETHESDA MD 20817-5700		8. PERFORMING ORGANIZATION REPORT NUMBER NSWCCD-61-TR-2006/01
9. SPONSORING / MONITORING AGENCY NAME(S) AND ADDRESS(ES)		10. SPONSOR/MONITOR'S ACRONYM(S)
		11. SPONSOR/MONITOR'S REPORT NUMBER(S)
12. DISTRIBUTION / AVAILABILITY STATEMENT Approved for public release		
13. SUPPLEMENTARY NOTES		

14. ABSTRACT

High-temperature tensile properties of pure rhenium metal were studied to better understand the material's behavior under load at elevated temperatures. Different processing procedures, particularly hot isostatically pressing (HIP) and diffusion bonding of cold-rolled plate, cause microstructure differences (grain size, porosity, texture) that significantly affect the resulting tensile properties. For this study, tensile specimens were tested at 2500 °F and characterized through extensive metallography and fractography. Results indicate rhenium is inherently ductile at 2500 °F with transgranular fracture being the dominant fracture mode. The HIPed specimens deform primarily through slip while the cold-rolled specimens deform through twinning. Additionally, the stress/strain properties of the HIPed material are consistently better than the cold-rolled plate.

Fracture toughness testing on cold-rolled rhenium plate was conducted at room temperature. Two plates of different thickness and grain sizes were tested per ASTM E 1820 and evaluated using Appendix A9: JIC and KJIC Evaluation. The two plates yielded significantly different results, likely due to the difference in the percent cold-work and grain size between the plates.

15. SUBJECT TERMS					
rhenium, microstructure characterization, deformation behavior, tensile, fracture toughness					

16. SECURITY CLASSIFICATION OF:			17. LIMITATION OF ABSTRACT	18. NUMBER OF PAGES	19a. NAME OF RESPONSIBLE PERSON Jennifer Gaies
a. REPORT UNCLASSIFIED	b. ABSTRACT UNCLASSIFIED	c. THIS PAGE UNCLASSIFIED	SAA	30	19b. TELEPHONE NUMBER *(include area code)* 301-227-5087

i/ii

This page intentionally left blank

Contents

Figures

Tables

Administrative Information

Acknowledgements

This page intentionally left blank

Executive Summary

High-temperature tensile properties of pure rhenium metal were studied to better understand the material's behavior under load at elevated temperatures. Different processing procedures, particularly hot isostatically pressing (HIP) and diffusion bonding of cold-rolled plate, cause microstructure differences (grain size, porosity, texture) that significantly affect the resulting tensile properties. For this study, tensile specimens were tested at 2500 °F and characterized through extensive metallography and fractography. Results indicate rhenium is inherently ductile at 2500 °F with transgranular fracture being the dominant fracture mode. The HIPed specimens deform primarily through slip while the cold-rolled specimens deform through twinning. Additionally, the stress/strain properties of the HIPed material are consistently better than the cold-rolled plate.

Fracture toughness testing on cold-rolled rhenium plate was conducted at room temperature. Two plates of different thickness and grain sizes were tested per ASTM E 1820 and evaluated using Appendix A9: J_{IC} and K_{JIC} Evaluation. The two plates yielded significantly different results, likely due to the difference in the percent cold-work and grain size between the plates.

Introduction

The unique properties of rhenium, such as high melting temperature (5756 °F), good combination of strength and ductility at high temperatures, and good resistance to oxidizing environments at high temperature, make rhenium the material choice for many high temperature applications [1]. In general, rhenium products are manufactured using powder metallurgy techniques followed by either hot isostatically pressing (HIP) or cold rolling. The cold-rolling process requires numerous cycles of deformation and annealing resulting in non-uniform grain structure and texture. As reported by Carlen and Bryskin [2] and Churchman [3], slip and twinning are the prominent deformation mechanisms during the cold-rolling process. In some applications, cold-rolled rhenium plates of different thickness are diffusion bonded, without the use of sintering additives, to satisfy complicated geometrical requirements.

Rhenium exhibits good, consistent room temperature tensile properties with tensile strengths greater than 100 ksi and elongation greater than 20%; however, considerable scatter exists in tensile properties when the testing temperature reaches 2500 °F, to which the causes are unknown. For the tensile behavior study, metallographic analyses were performed on two sets of diffusion-bonded cold-rolled rhenium plate and one group of HIPed specimens. In the two sets of cold-rolled plate, the specimens studied were chosen based on a significant difference in ductility (as measured by percent elongation). Three HIPed specimens were chosen to represent a range of tensile ductilities within the group of specimens. This investigation shows: 1) a strong correlation exists between the fracture mode and tensile elongation in both sets of cold-rolled plate where specimens with low ductility exhibit a band of intergranular fracture along one edge of the sample, and 2) cold-rolled specimens exhibit a significant degree of [0001] texture while the HIP specimens demonstrate little, likely leading to the higher ductility in the HIPed specimens.

The fracture toughness portion of this study was conducted to obtain insight into the fracture behavior of the material with a crack present. Prior to this testing, no fracture toughness data was available on pure rhenium metal. This study compares the behavior of two cold-rolled and annealed plates (different than those used in the tensile study) with different original thickness. The difference in thickness, caused by a difference in the number of cold-rolling and annealing procedures, led to different grain sizes in the material. This difference in grain size affected the fracture toughness behavior significantly, with the larger grain size material exhibiting better fracture toughness than the smaller grained material.

Materials Investigated

Tensile Specimens

Three sets of rhenium tensile specimens were investigated for this paper. Two of these sets of rhenium specimens were cold-rolled and diffusion-bonded specimens. In other words, several plates were cold-rolled to a thickness of 0.46 inch, ground to varying thickness, and subsequently diffusion bonded together (denoted CR1 and CR2). Tensile specimens were fabricated by welding rhenium tabs onto each end of the diffusion-bonded stack. An example of a tensile specimen is shown schematically in Figure 1, with the location of potential bond lines indicated on the tensile specimen. The rhenium tensile specimens were rolled, machined, and diffusion bonded in this manner to remain consistent with the production of the actual components. The third set of specimens was fabricated by sintering and hot isostatically pressing. The specimens originated from three separate 0.46-inch thick plates (denoted HIP1, HIP2, and HIP3) all processed identically, without any diffusion bonding. Similar to the cold-rolled tensile specimens, the HIPed tensile specimens were fabricated by welding tabs onto each end.
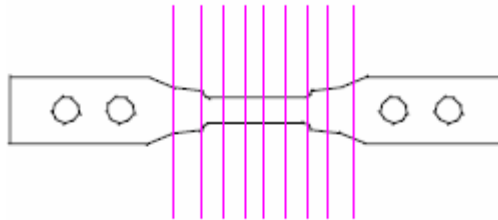
Figure 1: Schematic indicating the possible locations
of diffusion bond lines in the cold-rolled specimens

Tensile Properties

Southern Research Institute (SoRI) conducted tensile testing of the rhenium specimens. The specimens were tested in an inert atmosphere at a temperature of 2500 °F and at quasi-static rates. The fractured tensile specimens for each condition are shown in Figure 2. As shown in the photos, all of the cold-rolled specimens broke next to the tab radius while the HIPed specimens broke within the gage section. Coincidentally, a diffusion bond line is located at the tab radius for the cold-rolled specimens. Thus, an investigation into the cause of failure at the tab radius is discussed later in this paper.

The tensile strength and ductility are reported in Table 1 for the specimens that are analyzed in this report. For the cold-rolled group of samples, the specimens investigated were those with the largest difference in strain at fracture. For the HIPed specimens, those with the highest and lowest strain capabilities were considered, in addition to one with moderate strain at fracture. Based on these initial tensile results, the HIPed specimens exhibited significantly greater strength and ductility over the cold-rolled and diffusion-bonded specimens.
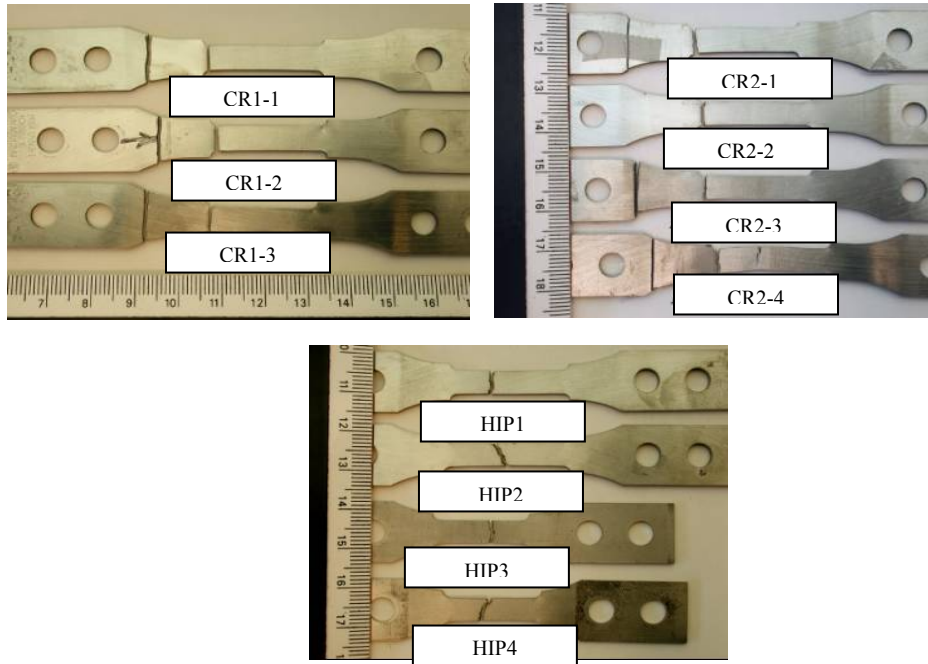
Figure 2: Macrographs of fracture tensile specimens

Table 1: Rhenium Tensile Properties at 2500 °F

Specimen	Ultimate Strength (ksi)	Yield Strength (ksi)	Strain at fracture (%)
CR1-1	36	23	11
CR1-3	26	22	3
CR2-1	27	22	4
CR2-4	33	22	11
HIP1	47	40	12
HIP2	47	36	17
HIP3	49	33	19.5

Fracture Toughness

Fracture toughness specimens were tested from two separate cold-rolled plates with thicknesses of 0.460 inches and 0.150 inches, respectively. Both plates originated from the same

size ingot; and thus, the thinner plate had significantly more cold-work and annealing cycles than the thicker plate. The exact processing details including the number of cold-rolling passes and annealing temperature are proprietary.

Approach

Tensile Specimens

The fracture surfaces of each specimen were examined using the scanning electron microscope (SEM) to determine the mode of failure and to observe any significant differences between each group of specimens. Following observations of the fracture surface, half of the broken tensile specimen was cross-sectioned through the center of the specimen, mounted, and polished. A schematic of the cross-sectioned tensile specimen is shown in Figure 3. The specimens were ground such that the "face" of the sample at the centerline could be observed directly at the fracture surface. The observations made on the cross-sectioned specimen focused on the crack path along the fracture surface (intergranular versus transgranular), microcracking below the surface, twinning, porosity, grain size, and bond lines (for specimens cold-rolled and diffusion bonded). Differences in any or all of these features can provide valuable insight into the cause of variation within plates of tensile specimens.
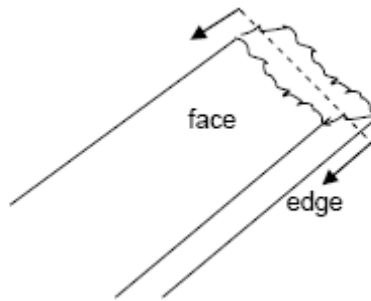
Figure 3: Schematic of cross-sectioned tensile
specimen for metallographic analysis

Fracture Toughness

Data obtained from previous room temperature rhenium tensile tests suggested plastic behavior would occur during fracture toughness testing. Therefore, ASTM E 1820: Fracture Toughness Testing of Metals was used in conjunction with *Appendix A9: J_{Ic} and K_{JIc} Evaluation* to increase the probability to obtain valid fracture toughness tests [4].

Initially, three specimens were machined from the 0.460-inch plate in the L-T orientation. The specimens were designed to be equivalent to 0.5-inch thick compact tension specimens (C(T)). The specimens were fatigue pre-cracked in air using load-shedding conditions. The final ΔK values ranged from 15.1 to 16.2 ksi√in, with the final crack sizes being 0.55 inch. Because the nominal thickness was less than 0.5 inch, the side grooves placed in the specimen after pre-cracking to promote straight ductile crack behavior were done to 7.4% of the original thickness on each side. This resulted in a specimen thickness of 0.4 inch, equivalent to a standard 0.5-inch

thick specimen. During testing of these three specimens, plastic instabilities occurred rendering the fracture toughness initiation (J_{IC}) values invalid.

After testing the first three specimens, it was apparent the toughness of the rhenium plate was low enough to allow for much thinner specimens; thereby, reducing material costs. Additionally, a thinner specimen with longer fatigue cracks would reduce the probability of plastic instabilities by increasing the compliance of the specimen. Hence, the remaining nine specimens were designed to have the same profile as the 0.5-inch thick C(T) specimen but with a thickness of 0.15 inch. A schematic of the specimen is shown in Figure 4. Of these final nine specimens, six were machined from the 0.460-inch plate and three from the 0.15-inch plate. All nine specimens were machined in the L-T orientation. The specimens were fatigue pre-cracked to a final crack length of 0.60 inch. The final ΔK values ranged from 20.0 to 21.8 ksi√in. These specimens were not side grooved because the low stresses required to fracture the material would result in straight ductile crack extensions without the aid of side grooves.

All twelve specimens were tested in a servo-hydraulic test system controlled with external software. Tests of the 0.5-inch thick specimens were controlled using a signal from the machine's linear variable differential transformer (LVDT) and a feedback loop in the computer. Tests of the 0.15-inch thick specimens were controlled using a transducer signal, which measured the crack mouth opening displacement. This slight change in testing resulted in a more sensitive system with the intention of reducing the chance of plastic instabilities occurring, as observed in the 0.5-inch specimens.
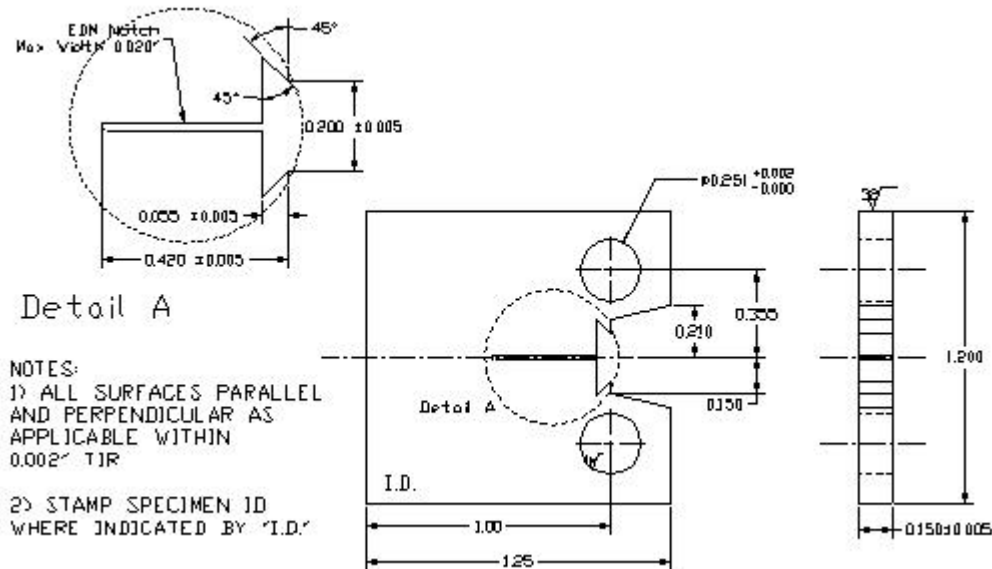
Figure 4: Drawing of the 0.150-in thick C(T) specimen

Results and Discussion

Tensile Specimens

Cold-rolled Specimens

A comparison was made between specimens CR1-1 and CR1-3. As reported in Table 1, the strain at fracture for CR1-1 was 11% and that for CR1-3 was only 3%. The fracture surfaces shown in

Figure 5 reveal a band of "rock candy" intergranular fracture exists along the edge of specimen CR1-3, while only ductile fracture is exhibited on specimen CR1-1.

(a)

(b)   **(c)**
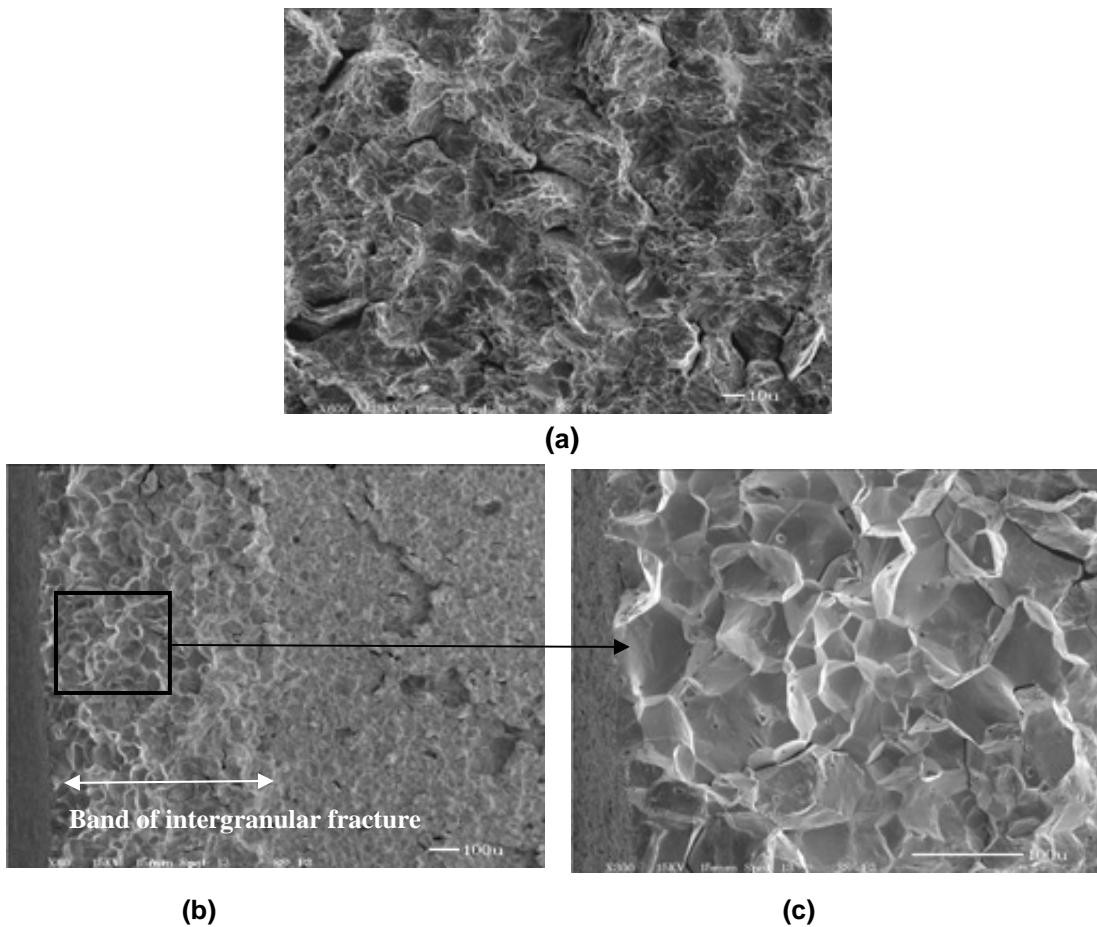
Figure 5: Fracture surfaces of CR1 rhenium tensile specimens: (a) fracture surface of CR1-1 showing ductile fracture characteristics, (b) and(c) fracture surface of CR1-3 showing a band of intergranular fracture approximately 800 microns in width

The cross-sectioned specimens further show intergranular fracture along the edge of the specimen with a mixed mode of transgranular/intergranular fracture across the remainder of the specimen. A micrograph of the cross-section of specimen CR1-3 is shown in Figure 6.

Significant damage can be seen below the fracture surface in the form of twinning, cracking, and recrystallized grains. The region of recrystallization developed due to the high temperature of testing (2500 °F) and the stresses during testing. A comparison of the microstructures for each specimen several millimeters from the fracture surface revealed specimen CR1-1 had significantly more twinning than specimen CR1-3. The limited twinning in specimen CR1-3 is due to its early yielding and failure as compared to CR1-1.

The location of the bond lines in relation to the fracture surface was determined by locating bond lines in the microstructure and comparing those with the plate thickness and stacking sequence. The fracture location was determined to be away from a bond line for specimen CR1-3, and either on or very near a bond line for specimen CR1-1. Therefore, because specimen CR1-1 showed good elongation even with a potential bond line failure, it is concluded the bond lines are not weak regions in the material. Additionally, no observation was made to indicate a different grain size or morphology existed next to the bond lines.

(a)   (b)
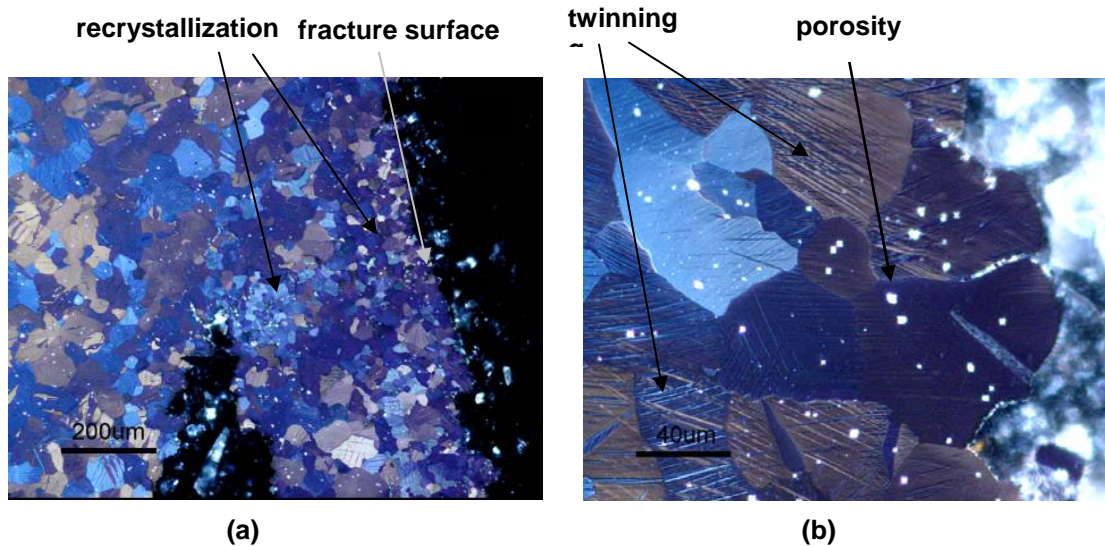
Figure 6: Cross-sectioned view of CR1-3 showing (a) recrystallized grains and cracking below the fracture surface and (b) intergranular fracture and twinning.

The specimens from plate CR2 are designated CR2-1 and CR2-4, with strain at fractures of 4% and 11%, respectively. Once again, the specimen with the lower ductility, CR2-1, exhibited a band of pure intergranular fracture along the edge of the specimen, much like that shown in

Figure 5. This band of intergranular fracture is approximately 600-800 microns in width, similar to that of the specimen from plate CR1. The remaining fracture region exhibited ductile fracture features. Cross-sections of each specimen are shown in Figure 7a and 7b. Specimen CR2-1 shows intergranular fracture and cracking, while specimen CR2-4 exhibits mainly transgranular fracture. In both micrographs, significant twinning and porosity is evident.

Once again, these specimens were analyzed to determine if the fracture occurred along a bond line, and for both specimens it was determined neither failed directly along a bond line. As noted previously and shown in Figure 2, all of the cold-rolled specimens broke at the tab radius. Coincidentally, a diffusion bond line is located directly next to the tab radius. The diffusion

bond lines tend to be weaker than the surrounding plate material. Therefore, it is likely that the combined effect of a bond line located at the tab radius as well as the higher stress concentration at the tab radius caused failures to occur in this location. Had the location of all bond lines been away from the tab radius, it is likely that failure would not have occurred next to the tab radius.
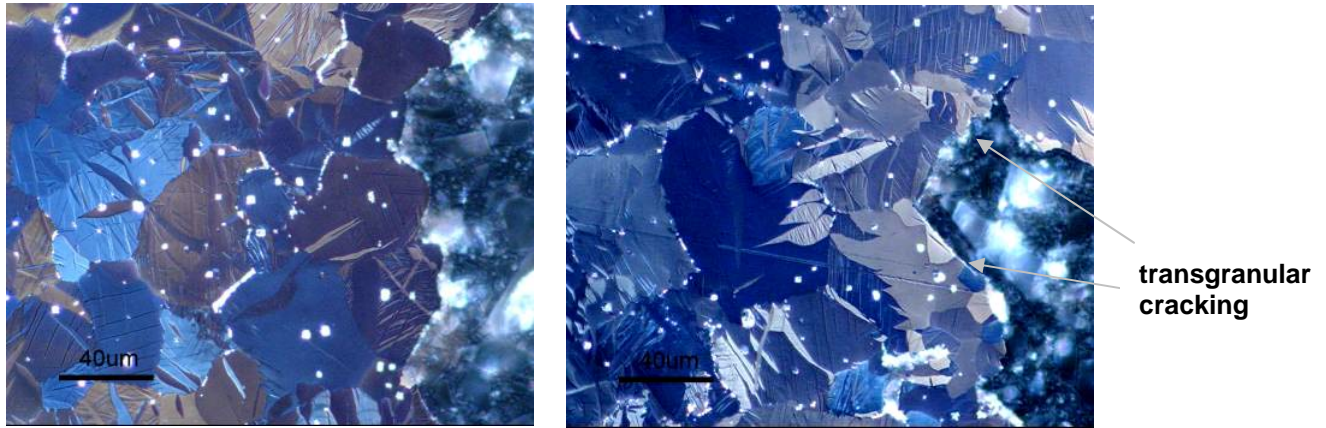
(a)   (b)

Figure 7: Cross-section micrographs of (a) CR2-1 showing intergranular fracture and (b) CR2-4 showing transgranular fracture

HIP Specimens

The final set of specimens studied were sintered and hot isostatically pressed. These specimens exhibited the greatest tensile strength and ductility at 2500 °F. An examination of the fracture surfaces and microstructures showed these specimens failed in a ductile manner with no indication of any intergranular failure, see Figure 8. Specimen HIP3 exhibited the most ductile fracture surface with typical microvoid nucleation, growth, and coalescence behavior. All of the HIPed specimens showed considerable cracking below the fracture surface, examples of which are shown in Figure 9. The numerous micocracks most likely formed after significant plastic deformation occurred in order to obtain elongations of 12-19.5%. The cracking occurred mostly along the grain boundaries, as seen in Figure 9b. Minimal twinning was observed in the grains indicating the dominant deformation mechanism in the HIPed specimens was slip.
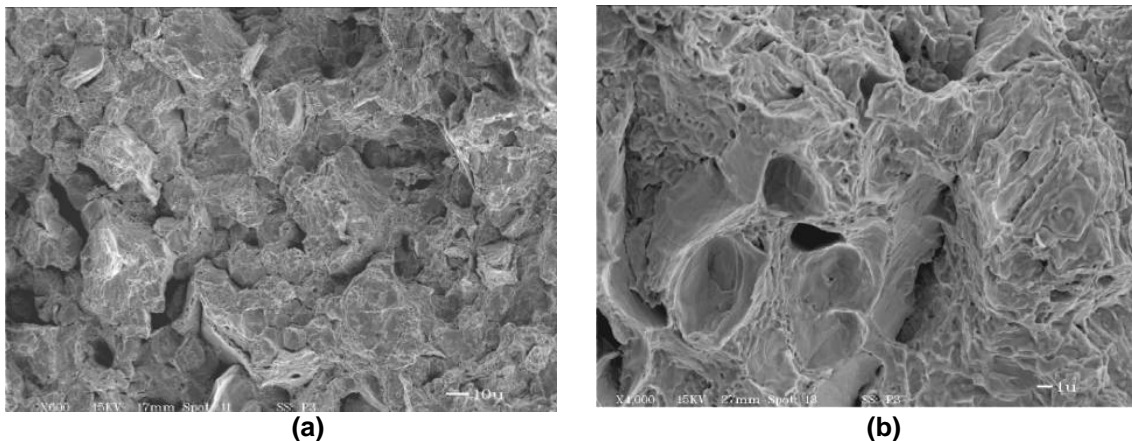
(a)   (b)

Figure 8: Fracture surfaces from the HIP tensile specimens (a) HIP1 (12% fracture strain) and (b) HIP3 (19.5% fracture strain) both showing ductile fracture

(a) (b)
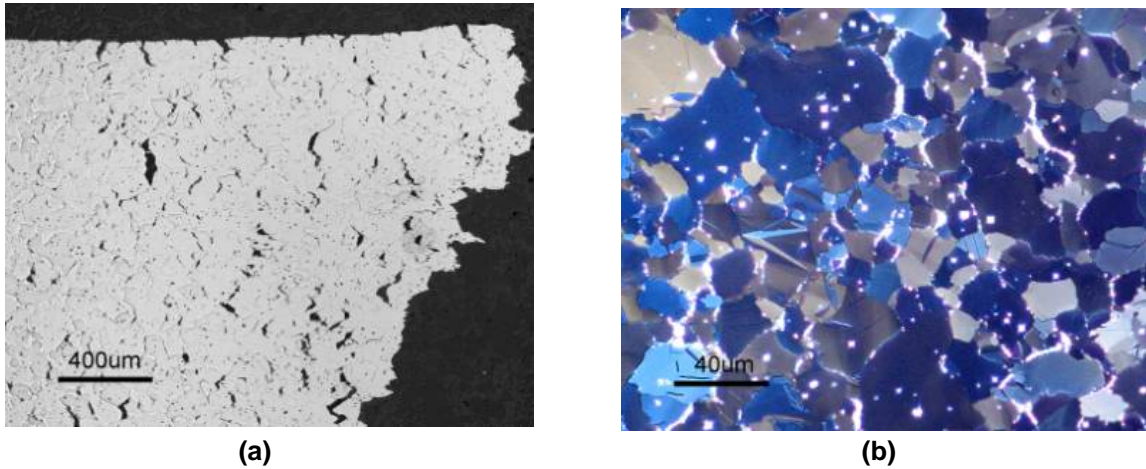
Figure 9: Cross-sectioned micrographs of specimen (a) HIP1 showing numerous cracks below the fracture surface and (b) HIP3 showing cracking along the grain boundaries

Cold-rolling vs. HIP

The previous discussion examined the behavior of each group of specimens individually and showed the HIPed specimens exhibited better tensile properties compared to the cold-rolled specimens. This behavior can be attributed to two differences, grain size and texture. Although quantitative grain sizes are not available for the two groups of specimens, the microstructures compared in Figures 7a and 9b qualitatively suggest the grain size in the HIPed specimens is significantly smaller than that of the cold-rolled specimens. Additionally, the grain size in the HIPed specimens varies considerably, from less than 10 μm to approximately 40 μm, as shown in Figure 10.

Previous unpublished studies by the authors on the effect of processing on texture revealed HIPed plate had little to no orientation preference while cold-rolled and annealed plate exhibited a moderate degree of planar [0001] texture (Figure 11). This texture occurs when grains prefer to orient with their [0001] direction lying parallel to the rolling direction. When texture develops, the number of grains oriented favorably for slip to occur is reduced, thus limiting the ductility of the material. Therefore, the texture in the cold-rolled material reduces the number of grains capable of slip decreasing the tensile properties of the rhenium material.

9
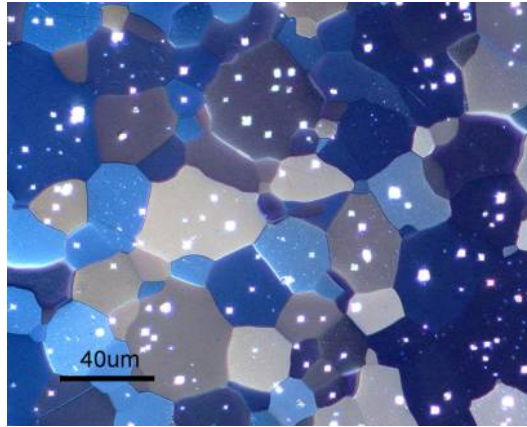
Figure 10: Grain size variation in HIP specimens

(a)   (b)
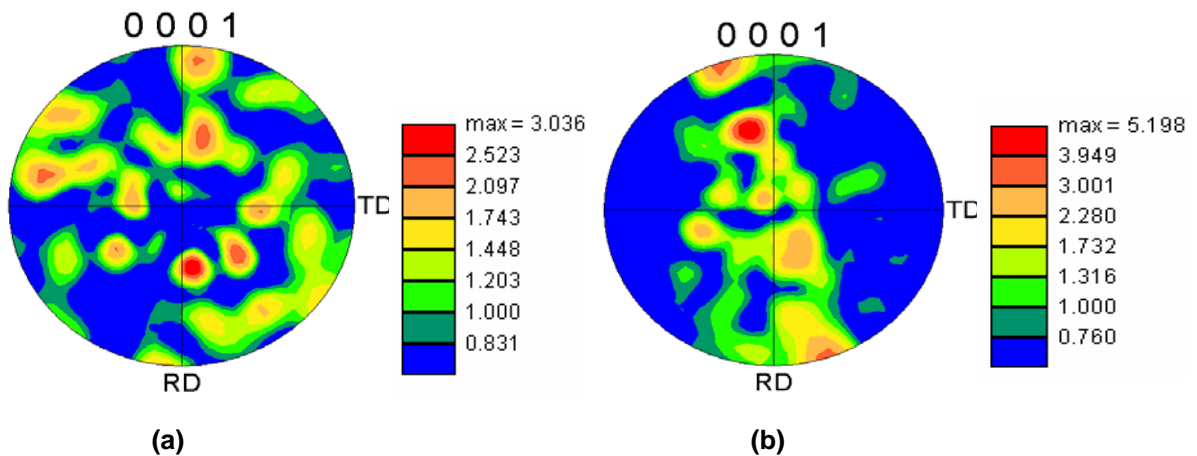
Figure 11: Texture plots on (a) HIPed and (b) cold-rolled plate showing the [0001]
preferred orientation of the grains in the cold-rolled plate

Fracture Toughness

The three initial tests conducted on 0.50-inch thick specimens were not used for comparisons because plastic instabilities initiated by the test setup and specimen size caused premature failure to occur in the samples.

Each plate thickness had consistent and distinct load-displacement curves. The 0.150-inch plate had a much higher resistance to tearing than the 0.460-inch plate. The average maximum loads of the two plates were 438 lbs and 473 lbs for the 0.460-inch and 0.150-inch plates respectively, as shown in Figure 12. However, the average crack mouth opening displacement (CMOD) required to obtain maximum load was 0.0170 inch and 0.0653 inch respectively. This factor of 3.8 between the CMOD to maximum load is an indication of the tearing resistance.

Another indication of the greater tearing resistance of the 0.150-inch plate is the slope of the J-R curve after crack initiation. The average dJ/da, where J is the crack initiation toughness and a is the crack length, after initiation for the 0.460-inch plate and the 0.150 inch plate are

3,746 lbs/in² and 19,517 lbs/in². This difference in tearing resistance, a factor of 5.2, can be seen in Figure 13.
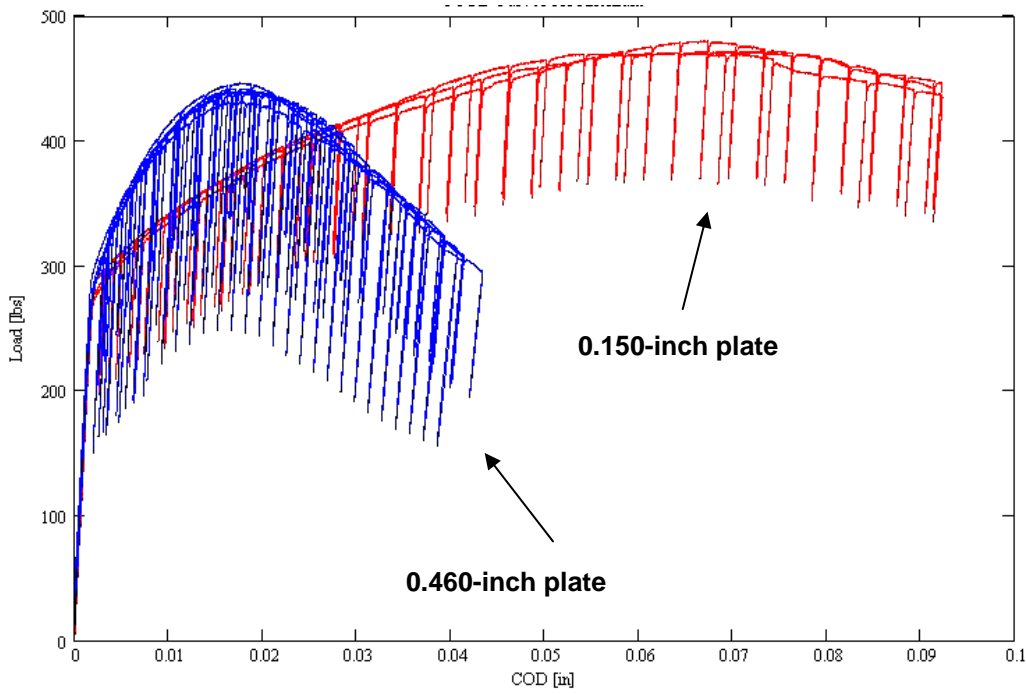

Figure 12: Representative load vs COD curves for each plate thickness
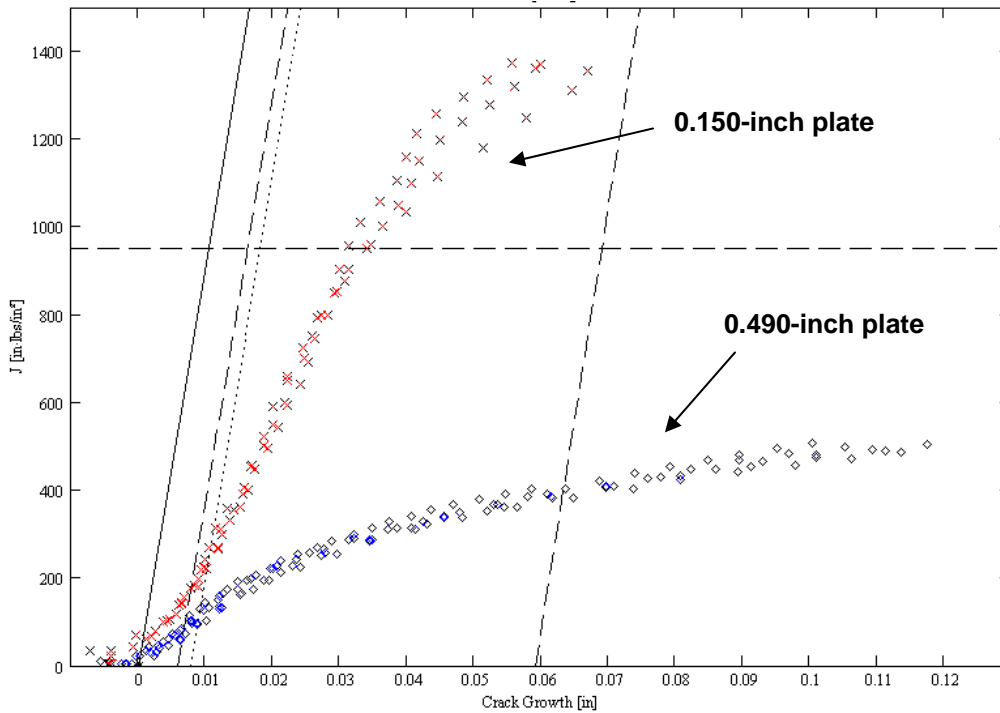
Figure 13: J-integral versus crack extension for each plate thickness

The values of critical crack initiation toughness (J_{IC}) obtained using the J-integral technique also show two distinct populations. The 0.460-inch plate had an average initiation toughness of 134 in·lb/in². This value is 3.4 times lower than the average initiation toughness of the 0.150-inch plate, 469 in·lbs/in². The results are given in Table 2.

Specimens 1, 2, and 3 were the specimens tested with a thickness of 0.50 inch. These J_Q values are considered invalid J_{Ic} values due to the plastic instabilities caused by the test setup. These instabilities made a final estimation of the crack size using the compliance method impossible. The three additional invalid J_{Ic} tests are also considered invalid because of incorrect estimations in the final crack length. However, the data were still used in the reported averages because: the invalidities were not due to plastic instabilities, the values of J_Q are statistically identical to the qualified J_{Ic} values, and the load-CMOD and J-R curves are consistent. The average results and standard deviations are displayed graphically in Figure 14.

Table 2: Tabular J-Integral Results

| Specimen ID	Plate Thickness (in)	Specimen Thickness (in)	J_Q (in-lb/in^2)	Valid J_{IC}?	Why Not Valid?
1			120	No	Error in crack extension prediction
2		0.50	107	No	Error in crack extension prediction
3			140	No	Error in crack extension prediction
4	0.460		144	Yes	
5			137	Yes	
6			177	Yes	
7			135	No	Error in crack extension prediction
8		0.150	136	Yes	
9			145	No	Error in crack extension prediction
1A			478	Yes	
2A	0.150		442	No	Error in crack extension prediction
3A			486	Yes	
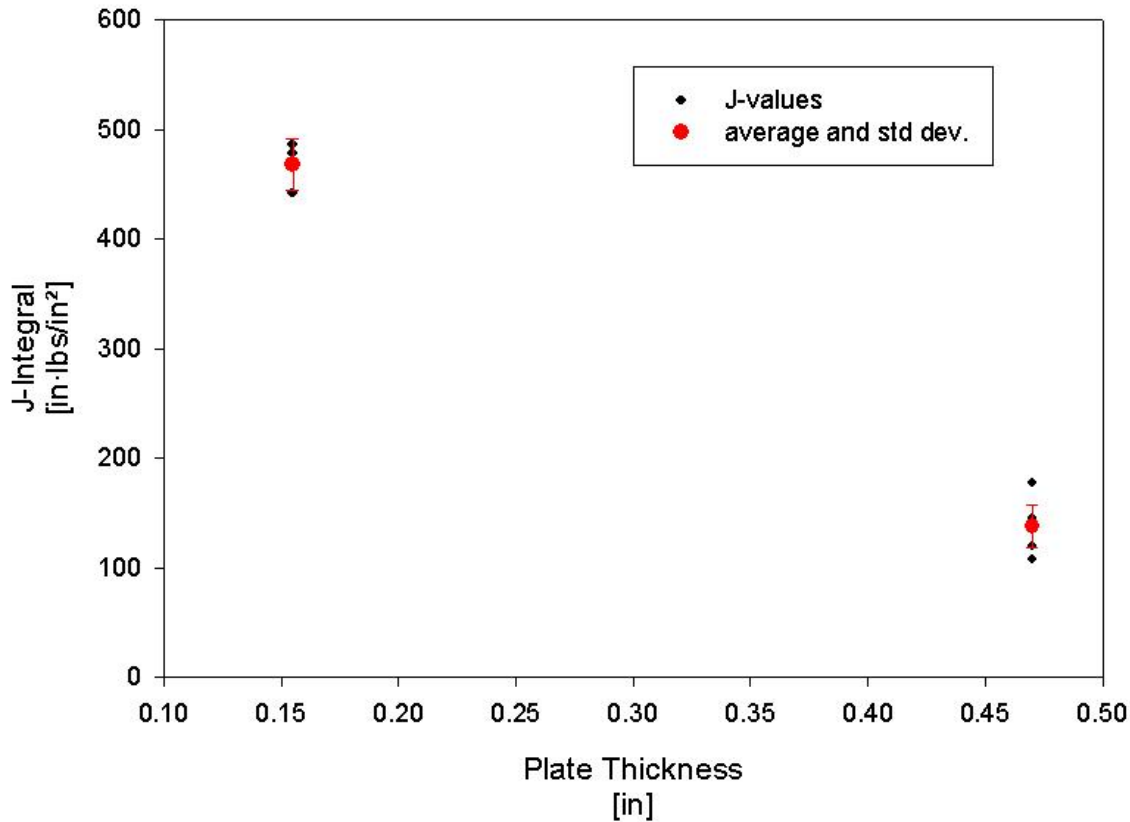
Figure 14: J-integral vs plate thickness

To understand the microstructural difference between the two plates, fractography was conducted on the fracture toughness specimens. The method of failure for both plates was predominately intergranular fracture, despite some plasticity. Both the fatigue pre-crack region and the ductile crack extension regions exhibited the same failure mechanisms. One significant difference between the plates is the grain size. The 0.460-inch plate has a grain size on the order of 10 μm, while the 0.150-inch plate has a grain size on the order of 100 μm. The grain size difference is due to the different number of cold-rolling and annealing cycles each plate underwent. Figure 15 depicts the fracture surfaces from the ductile extension region of each plate. Figure 15 (a) and (b) are taken at the same magnification to show the drastic difference in grain size between the two plates. Figure 15 (c) and (d) show each plate failed in a uniform manner with intergranular fracture as the dominant failure mechanism. Traditionally, material with a smaller grain size tends to have better fracture toughness than the same material with a larger grain size. Pure rhenium metal does not appear to follow this theory, and this may be attributed to the intergranular fracture mode. If the weakest site in the material is on the grain boundaries, then a larger grain size leads to a lower volume fraction of grain boundaries or "weak regions" in the material. Further investigations are needed to better understand the effect of grain size on the fracture toughness behavior of pure rhenium metal.

13

Specimens from each plate were cross-sectioned to examine the extent of secondary out-of-plane cracking. The out-of-plane cracking was less than one grain in length; thus, the continuum mechanics assumptions made in fracture toughness testing remain valid.

An additional material difference between the two plates is texture. It is likely the thinner plate, which received more work, has more induced texture than the thicker plate. However, orientation imaging microscopy could not be completed at this time to determine the extent of texture in each plate.
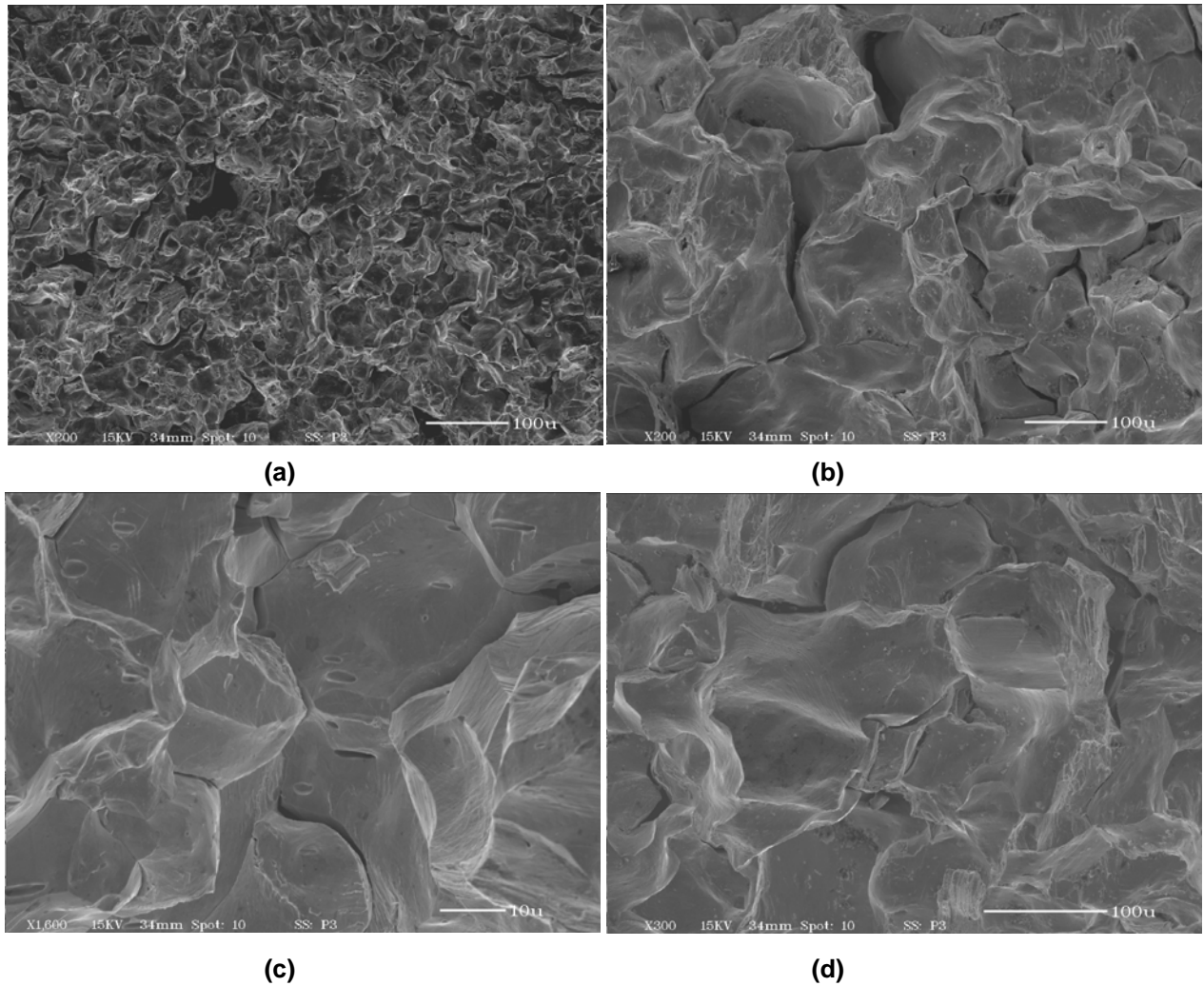

Figure 15: Fracture surface of (a) 0.490-inch thick plate at 200x (b) 0.150-inch thick plate at 200x showing grain size differences and (c) 0.490-inch thick plate at 1600x (d) 0.150-inch thick plate at 300x showing similar fracture features from each plate

Conclusions

This study examined the tensile behavior of pure rhenium cold-rolled and diffusion-bonded specimens and hot isostatically pressed (HIPed) specimens. In general, the HIPed specimens had greater strength and ductility than the cold-rolled and diffusion-bonded specimens with the best ultimate strength/elongation combinations of 49 ksi / 19.5% for HIPed specimens and 36 ksi / 11% for cold-rolled and diffusion-bonded specimens. This difference was attributed to lower degree of texture in the HIPed specimens and possibly differences in grain size.

The variation in ductility within each group of cold-rolled and diffusion-bonded specimens is a result of a band of intergranular fracture along the edge of each specimen with lower fracture strains. The cause of intergranular fracture on those particular specimens and its occurrence in a band along the edge of the specimen is unknown. Further investigations need to be conducted to fully understand the origin of intergranular fracture.

The fracture toughness test results showed significant differences in the toughness between the 0.460-inch thick plate and the 0.150-inch thick plate. The thicker plate had an average initiation toughness of 134 in-lb/in^2 while the thinner plate had an average initiation toughness of 469 in-lb/in^2. Fractography indicated both plates failed intergranularly. A likely cause for the difference in fracture toughness behavior is the grain size difference between the plates. The 0.490-inch thick plate had a grain size of approximately 10 μm while that of the 0.150-inch thick plate was approximately 100 μm. This difference in grain size can be attributed to the difference in the number of cold-rolling and annealing cycles each plate received. The thinner plate underwent more cold rolling and annealing treatments than the thinner plate, thus, causing the thinner plate to have a larger grain size. Effects of texture differences between these two plates were not considered in this study, but could provide useful information in the future.

References

1. B.D. Bryskin, "Rhenium and Its Alloys," *Advanced Materials Processing*, September 1992, pp. 22-27.

2. J.C. Carlen and B.D. Bryskin, "Cold Froming Mechanisms and Work Hardening Rate for Rhenium," *Metallic High Temperature Materials*, Vol. 1, ed. by H. Bildstein and R. Eck, Plansee Proceedings, 1993, pp. 79-92.

3. A. T. Churchman, "Deformation Mechanisms and Work hardening in Rhenium," *Trans. AIME*, Vol. 218, April 1960, pp. 262-267.

4. E1820-02 Standard Test Method for Measurement of Fracture Toughness, *American Society for Testing and Materials*, 2004.

Distribution

	copies			copies
		RHENIUM ALLOYS, INC.		
		TODD LEONHARDT		1
		1329 TAYLOR STREET		
DOD - CONUS		P.O. BOX 245		
		ELYRIA, OH 44036		
CHIEF OF NAVAL RESEARCH				
ATTN ONR 332 (J. CHRISTODOULOU)	1			
BALLSTON CENTRE TOWER ONE		HONEYWELL		
800 NORTH QUINCY ST		SCOTT SPERL		1
ARLINGTON VA 22217-5660		1300 W. WARNER RD		
		P.O. BOX 22200		
COMMANDER		TEMPE, AZ 85285		
NAVAL SEA SYSTEMS COMMAND				
ATTN SEA 05M	1			
1333 ISAAC HULL AVE SE STOP 5130		**INTERNAL DISTRIBUTION**		
WASHINGTON NAVY YARD DC 20376-5130				
		CODE 60		1
		CODE 61		1
COMMANDER		CODE 611		1
NAVAL SEA SYSTEMS COMMAND		CODE 611	(WELLS)	1
ATTN SEA 05M2 (G. MITCHELL)	2	CODE 612		2
1333 ISAAC HULL AVE SE STOP 5132		CODE 612	(CZYRYCA)	1
WASHINGTON NAVY YARD DC 20376-5132		CODE 612	(FIELDER)	1
		CODE 612	(FOCHT)	1
COMMANDER		CODE 612	(GAIES)	2
NAVAL SEA SYSTEMS COMMAND		CODE 612	(HAYDEN)	1
ATTN SEA 05P2 (J. A. MANUEL)	1	CODE 612	(MERCIER)	1
1333 ISAAC HULL AVE SE STOP 5142		CODE 612	(MOUSSOUROS)	1
WASHINGTON NAVY YARD DC 20376-5142		CODE 612	(PURTSCHER)	1
		CODE 612	(RAO)	1
		CODE 612	(ROE)	1
DEFENSE TECHNICAL INFORMATION CTR		CODE 612	(ROBINSON)	5
8725 JOHN KINGMAN ROAD SUITE 0944		CODE 612	(SANDERS)	1
FORT BELVOIR VA 22060-6218	1	CODE 612	(STILES)	1
		CODE 612	(SUTTON)	1
NoN-DoD		CODE 612	(SYLVESTER)	1
		CODE 612	(ZHANG)	2
SOUTHERN RESEARCH INSTITUTE		CODE 613		1
SAMUEL J. CAUSEY	1	CODE 614		1
757 TOM MARTIN DRIVE		CODE 615		1
BIRMINGHAM, AL 35211		CODE 616		1
		CODE 617		1
MATERIALS ENGINEER		CODE 617	(OPEKA)	2
SOUTHERN RESEARCH INSTITUTE		CODE 3442	(TIC-pdf only)	1
RANDALL S. JENKINS	1			
757 TOM MARTIN DRIVE				
BIRMINGHAM, AL 35211				
YING KO	1			
ATK				
55 THIOKOL RD				
ELKTON, MD 21921				

Distribution

copies	*copies*

This page intentionally left blank

Carderock Division